Macromolecules
ARTICLE

*Macromolecules* **2010**, *43*, 1035–1040 **1035**
DOI: 10.1021/ma902250d

# Depression of the Zero Growth Temperature by Counits Observed for *s*-Polypropylene in Light Attenuation Experiments

**Ralf Delto,[†] Werner Stille, and Gert Strobl***

*Physikalisches Institut, Albert-Ludwigs-Universität Freiburg, 79104 Freiburg, Germany.*
*[†] Present address: Areva NP, 91052 Erlangen.*

*Received October 15, 2009; Revised Manuscript Received November 26, 2009*

ABSTRACT: The growth rate of polymer crystals decreases exponentially with rising temperature, thus indicating a growing activation barrier. The barrier is proportional to the inverse of the supercooling below the "zero growth temperature" $T_{zg}$, which is always located below the equilibrium melting point. In order to see the effect of counits on $T_{zg}$, we studied with time-dependent light attenuation measurements the growth kinetics of *s*-polypropylene and a derived statistical copolymer with 15% of octene counits. Using a home-built device, we achieved a sensitivity superior to DSC or X-ray experiments. An accurate extrapolation procedure yielded for both samples the zero growth temperature. The counits lead to a downward shift of $T_{zg}$ by 40 K, which is larger than the downward shift of the melting point (30 K). We interpret the results in the framework of our multistage model which assumes participation of a transient mesophase in the growth process of polymer crystals. $T_{zg}$ is identified with the equilibrium melting point of the mesophase. Knowledge of $T_{zg}$ allows to establish for both samples a size−temperature nanophase diagram. Data evaluation yields the heat of melting and the surface free energy of mesomorphic layers as well as the activation barrier per monomer.

## 1. Introduction

On cooling a polymer melt, platelike crystals are nucleated and grow in the two lateral directions. The final structure is semicrystalline and composed of stacks of such crystallites separated by entangled fluid chain sequences. For long time it was generally assumed that both the thickness and the growth rate of the crystals are determined by the supercooling below the equilibrium melting temperature $T_f^\infty$.[1] During the past decade understanding changed. Experiments on several polymer systems, first of all carried out by time- and temperature dependent X-ray scattering experiments, contradicted the previous assumptions and demonstrated that crystallization and melting of bulk polymers are controlled by the distances to three different temperatures:[2,3]

• The crystal thickness $d_c$ varies with the inverse of the supercooling below a characteristic temperature $T_c^\infty$

$$d_c^{-1} = C_c(T_c^\infty - T) \tag{1}$$

$T_c^\infty$ is always higher than $T_f^\infty$.

• The crystal growth rate $G$ is given by

$$G = G_0 \exp\left(-\frac{T_A}{T - T_V}\right) \exp\left(-\frac{T_G}{T_{zg} - T}\right) \tag{2}$$

The first exponential term expresses the temperature dependence of the segmental mobility in the melt, $T_A$ and $T_V$ denoting the activation temperature and the Vogel temperature. The second exponential factor in the equation describes an activated process with a barrier height which diverges at the "zero growth temperature" $T_{zg}$. For all investigated systems $T_{zg}$ is located below $T_f^\infty$.

*Corresponding author. E-mail: strobl@uni-freiburg.de.

• The equilibrium melting temperature $T_f^\infty$ is the theoretical melting point of a perfect macroscopic polymer crystal. The platelike crystallites formed upon cooling a polymer melt have thicknesses in the nanometer range and therefore depressed melting points $T_f$. These are given by the Gibbs−Thomson equation as

$$T_f = T_f^\infty - \frac{2\sigma_e T_f^\infty}{\Delta h_f}\frac{1}{d_c} \tag{3}$$

$\sigma_e$ and $\Delta h_f$ denote the excess free energy of the fold surface and the heat of fusion, respectively.

For the use of polymeric materials it is important to know the effect of counits on crystallization and melting processes. Experiments have shown that, for a fixed crystallization temperature, the crystal thickness is an invariant property; i.e., eq 1 holds commonly for homopolymers and copolymerized derivatives with unique values of $T_c^\infty$ and $C_c$.[4,5] On the other hand, it is common knowledge that the inclusion of counits depresses the melting point and results in a decrease of the growth rate at a given temperature. Up to now nothing is known about the influence of counits on the zero growth temperature, the main parameter in control of the growth rate. We took up this question and carried out appropriate experiments. The results are presented in this publication.

Determinations of zero growth temperatures so far were performed by measuring in a polarizing optical microscope the growth rate of a selected spherulite at a series of stepwise increasing temperatures. We obtained accurate values for poly(ε-caprolactone),[6] polyethylene,[7] and *s*-polystyrene.[2] About 10 years ago we investigated by small-angle X-ray scattering the crystallization properties of *s*-polypropylene and several derived octene copolymers.[4] Figure 1 shows for two of the samples the homopolymer (sPP) and one copolymer (sPPcO15, it includes 15% per weight of octene units), the dependence of the (inverse)


Published on Web 12/11/2009

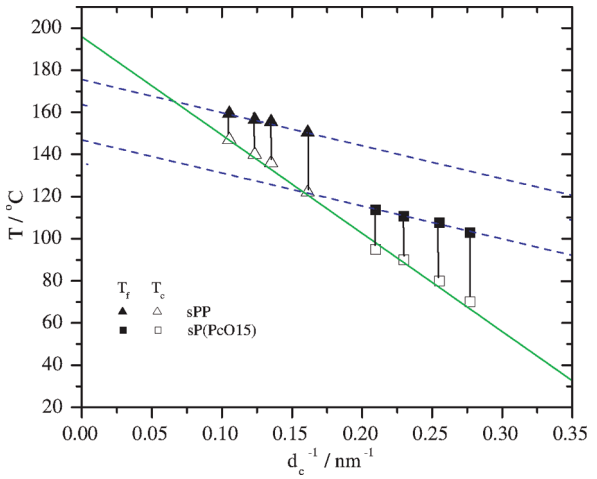


**Figure 1.** sPP and sPPcO15: dependence of the inverse crystal thickness $d_c^{-1}$ on the crystallization temperature (open symbols located on the crystallization line). Variation of the melting points of sPP (triangles) and sPPcO15 (squares) with $d_c^{-1}$ (filled symbols located on the two melting lines). From ref 4.

crystal thickness on the crystallization temperature as given by the linear relationship eq 1, and the variation of the melting points with $d_c^{-1}$ according to eq 3. Extrapolation of the "crystallization line" yields $T_c^{\infty} = 195$ °C; extrapolation of the "melting lines" gives $T_f^{\infty} = 176$ and 147 °C for sPP and sPPcO15, respectively.

We now used these two samples again for a determination of zero growth temxperatures. For sPP and its derivatives it is not possible to directly measure the growth rate of an isolated spherulite in a polarizing microscope as done previously. They form at high crystallization temperatures hedrites[8] with diffuse boundaries. An appropriate technique to deal with such a situation is time-dependent light attenuation measurement, carried out at various crystallization temperatures. An additional advantage of this technique is its high sensitivity, giving signals already in the initial stages of the crystallization process, much earlier than conventional techniques. We used a home-built special device which we had first successfully applied to crystallizing polyethylene and the crystallization of a commercial sPP with low tacticity.[9]

In the following we explain at first the principles of light attenuation measurements and the device construction. Next the procedure used in the determination of $T_{zg}$ is described, and the results are presented. We understand the appearance of three different controlling temperatures in the laws describing polymer crystallization and melting as evidence for the participation of a transient mesomorphic phase and developed a "multistage model". It assigns the three controlling temperatures to the equilibrium transition temperatures between melt, mesophase, and crystal. The absence of counit effects on the crystallization line indicates an exclusion of the counits from the mesophase—they are already rejected at the melt−mesophase interface. With the knowledge of $T_{zg}$ a size−temperature nanophase diagram can be established which allows in particular a derivation of properties of the mesomorphic phase. The results of a data evaluation based on the multistage model are presented in the last section.

## 2. Light Attenuation by Crystallizing Polymers

**2.1. Principles of the Technique.** While polymer melts are as transparent as all fluids and a light beam passes through with only negligible losses in intensity, nucleation and growth of spherulites or hedrites as it sets in after a cooling into the crystallization range is always accompanied by a rising attenuation. For a platelike sample with thickness $D$, it is described by the Lambert−Beer law

$$\frac{I}{I_0} = \exp(-\Lambda D) \tag{4}$$

$I_0$ denotes the flux of the light beam at the sample front, and $I$ gives the flux behind the sample. The parameter $\Lambda$ is the linear attenuation coefficient. By carrying out a time-dependent measurement of $\Lambda$

$$\Lambda(t) = \frac{1}{D} \ln \frac{I(0)}{I(t)} \tag{5}$$

it is possible to monitor the crystallization process. First uses of this techniques were described already long ago,[10−13] but it did not become a standard procedure. Derivation of quantitative results through the whole crystallization process is difficult. On the other hand, the technique has a high sensitivity, superior to the established standard tools calorimetry, dilatometry, or X-ray scattering. While the latter begin the detection of spherulites only at sizes above several hundred nanometers, the attenuation begins to rise much earlier. Exactly during these early stages the situation remains simple. The scattering objects are randomly distributed in dilute fashion and scatter the light independently. Under such conditions $\Lambda$ can be related to properties of the individual scatterers and described as

$$\Lambda = \rho\sigma^2 \tag{6}$$

Here $\rho$ denotes the number density and $\sigma^2$ the total scattering cross section of the objects. Three different ranges exist in dependence of the object size $R$, the refractive index of the objects $n_s$, and the refractive index of the fluid matrix $n_m$. Using the parameters

$$m = \frac{n_s}{n_m} \tag{7}$$

and

$$\alpha = \frac{2\pi n_m R}{\lambda_v} \quad (\lambda_v\text{: wavelength of the light beam in vacuo}) \tag{8}$$

these are the regimes of (i) Rayleigh scattering, for $\alpha < 1$, (ii) Rayleigh−Debye−Gans scattering, for $1 < \alpha < (m-1)^{-1}$, and (iii) Mie scattering, for $\alpha > (m-1)^{-1}$. Explicit expressions for $\sigma^2$ in the three ranges are given in the literature, first of all for spheres with a homogeneous inner structure.[14] Characteristic power laws hold in the centers of the three ranges: (i) for Rayleigh scattering the power law $\sigma^2 \propto R^6$, (ii) for Rayleigh−Debye−Gans scattering the law $\sigma^2 \propto (m-1)^2 R^4$, and (iii) for Mie scattering the law $\sigma^2 \propto R^2$. There exists an analytical expression for both the Rayleigh and the Rayleigh−Debye−Gans range which can be directly applied. Mie scattering relationships are more involved. However, during the initial stages of a polymer crystallization process the Mie range is not yet reached. Furthermore, the Rayleigh range is often already left when observations start, so that one usually can refer to the laws valid for the Rayleigh−Debye−Gans regime solely.

In the ideal case of a constant number of spherulites with a homogeneous, already fully established inner structure,

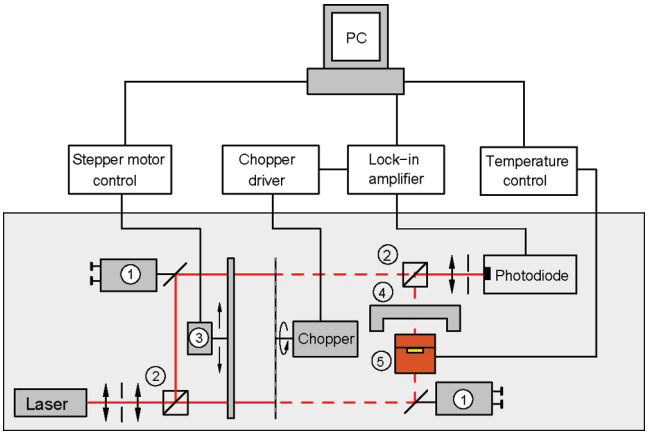


**Figure 2.** Experimental setup for light attenuation measurements: 1, adjustable mirrors; 2, beam splitters; 3, selective beam attenuator; 4, heat shield; 5, sample oven.

growing with a constant rate, the result expected for $\Lambda$ in a temperature-dependent experiment thus is

$$\Lambda \propto t^4 \tag{9}$$

Often the inner structure is time-dependent, with filling-in and perfectioning processes following up with some delay.[15] Then the law describing the evolution of $\Lambda$ during the initial stages deviates from eq 9 and generally reads

$$\Lambda \propto t^{\nu} \tag{10}$$

**2.2. Experimental Setup.** The light attenuation measurements were carried out using a chopper modulated two-beam setup together with lock-in signal detection. The device, built in the workshop of our institute, is displayed schematically in Figure 2.

An intensity-stabilized semiconductor laser module is utilized as light source (Global Lasertech; wavelength 635 nm, power 5 mW). After passing a spacial filter the laser beam is split into two beams of equal intensity: one passing through the sample and the other being led around the sample and serving as reference. At the beginning of the experiment, when the sample is in the melt state, an intensity match of sample beam and reference beam is carried out by attenuating one or the other with the aid of a beam attenuator. Both beams are directed onto a chopper which lets pass only one beam at a time. After passage through the sample contained in an oven, a second beam splitter recombines the sample beam with the phase inverted reference beam. The conjunct beam is focused on a pinhole and directed onto a photodiode. The signal is registered by a lock-in amplifier working at the chopper frequency (Stanford Research Systems model SR830). It is proportional to the intensity difference between sample and reference beam. Data of the time-dependent measurements are stored in a computer for further evaluation. Detailed information about the setup is included in ref 16.

As a demonstration of the device performance, a crystallization isotherm of a commercial sPP is displayed in Figure 3 and compared to an isotherm obtained by dilatometry.

The improvement of the sensitivity resulting in an extension of the observed period of crystallization by nearly 1 order of magnitude is obvious.

## 3. Determination of Zero Growth Temperatures

In a light attenuation experiment the growth kinetics of spherulites, hedrites, or other objects during the initial stages of

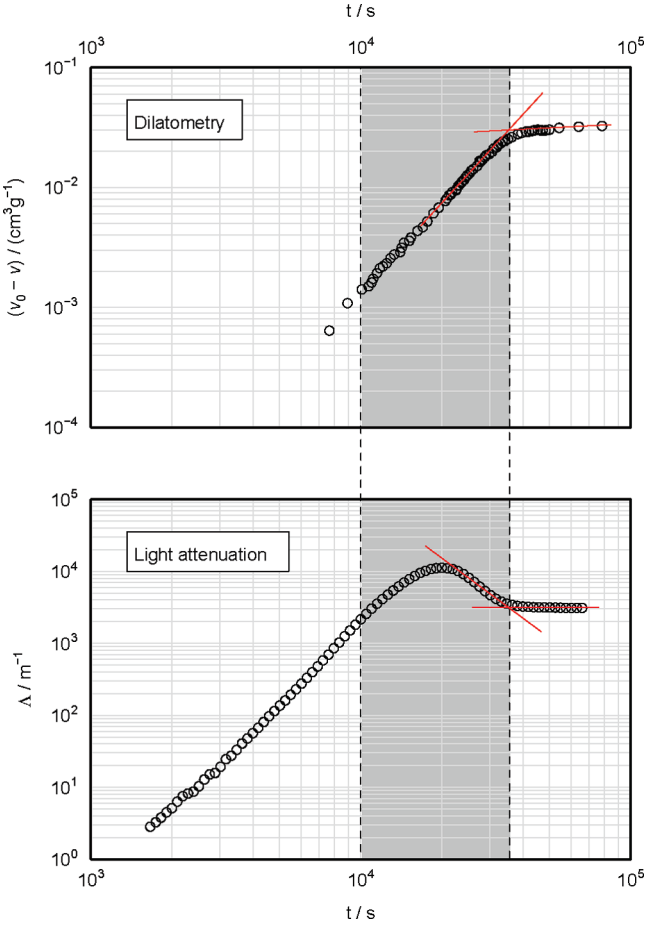


**Figure 3.** Comparison of two crystallization isotherms of a commercial sPP at 115 °C, obtained by dilatometry and light attenuation.

crystallization shows up in the time dependence $\Lambda(t)$ according to eq 10. If we include a rate constant $u$, it has the form

$$\Lambda \propto (ut)^{\nu} \tag{11}$$

$u$ varies with temperature in the same manner as the growth rate of the crystallites which compose the objects, i.e., according to eq 2 as

$$u = u_0 \exp\left(-\frac{T_A}{T - T_V}\right) \exp\left(-\frac{T_G}{T_{zg} - T}\right) \tag{12}$$

In order to determine the zero growth temperature, the rate constant $u$ given by the slope

$$u = \frac{d\Lambda^{1/\nu}}{dt} \tag{13}$$

has to be determined at a series of increasing temperatures. Starting from eq 12, a differentiation of ln $u$ with regard to $T$ followed by some reordering leads directly to

$$\left(-\frac{d \ln(u/u_0)}{dT} + \frac{T_A}{(T_V - T)^2}\right)^{-1/2} = T_G{}^{-1/2}(T_{zg} - T) \tag{14}$$

Using this equation, $T_{zg}$ can be obtained by a linear extrapolation based on measured values of the temperature derivative $d \ln(u/u_0)/dT$. One might first think that time-dependent

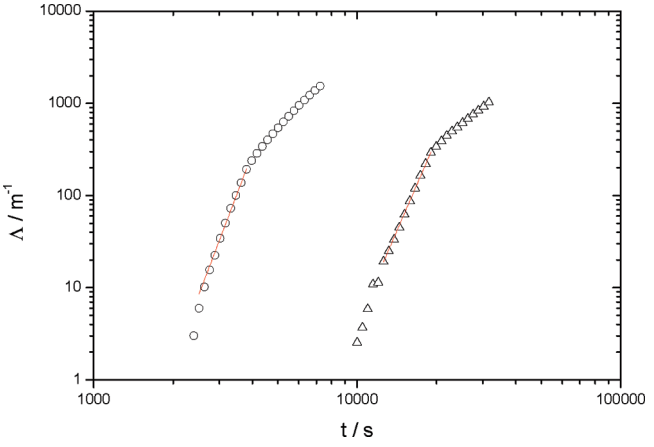


**Figure 4.** sPPcO15: time dependence of Λ during a crystallization at 82 °C followed by a jump to 87 °C (circles) and at 92 °C followed by a jump to 97 °C (triangles).

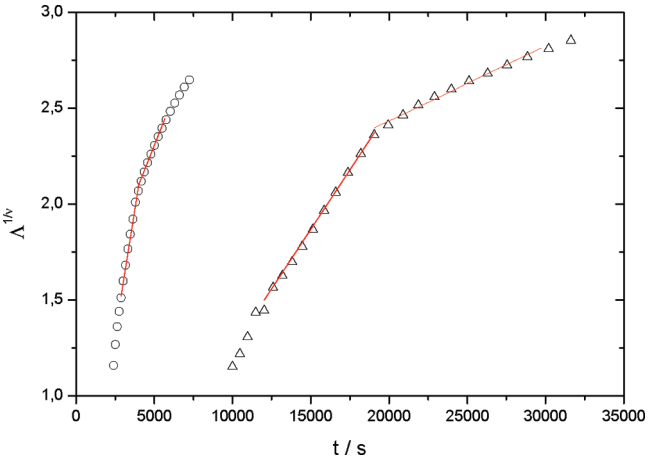


**Figure 5.** Time dependence of $\Lambda^{1/7.5}$.

measurements of Λ at a series of temperatures provide the required knowledge. However, considering eq 6, this is not strictly true since the number density of objects, although constant in time in the given case of heterogeneous nucleation, might vary with temperature. There is a better procedure: The experiment is started at a certain crystallization temperature $T_c$ and then continued after a upward temperature jump $\Delta T$. An upward temperature jump leaves the number of growing objects constant and affects the object growth rate only. The temperature derivative in eq 14 then follows from

$$-\frac{\mathrm{d}\ln(u/u_0)}{\mathrm{d}T} \approx -\frac{\Delta\ln(u/u_0)}{\Delta T} = -\frac{1}{u}\frac{\Delta u}{\Delta T} \qquad (15)$$

An example is provided with Figures 4 and 5. They represent the result of measurements on sPPcO15 at starting temperatures $T_c = 82$ and 92 °C, continued by a temperature jump $\Delta T = 5$ K. Figure 4 demonstrates that $\Lambda(t)$ indeed obeys a power law, here with an exponent $\nu = 7.5$. The temperature jump was carried out within the region of the initial power law, thus ensuring that the growing objects were still isolated. The jump results in a break.

Figure 5 presents a plot of $\Lambda^{1/\nu}$ vs $t$. The slopes before and after the break give according to eq 13 the respective values of $u$, thus yielding the temperature derivative $\Delta u/\Delta T$.

## 4. Experimental Results

Samples with a thickness of about 100 μm were kept between two glass slides. In order to remove all memory effects, they were first annealed at 200 °C on an external hot stage for some minutes and then rapidly transferred into the sample oven preset at the crystallization temperature. Measurements started immediately after the transfer. The cooling process was completed within less than 30 s; in the temperature ranges of interest first crystallization signals were detected only after more than 1000 s so that the cooling period is irrelevant. The increase of Λ was followed in real time. When values of about 300 $m^{-1}$ were reached, the temperature was increased by $\Delta T = 5$ K. For both samples, sPP and sPPcO15, kinetic measurements were carried out for a series of increasing crystallization temperatures $T_c$. Measurements at the highest temperature lasted for about 10 h.

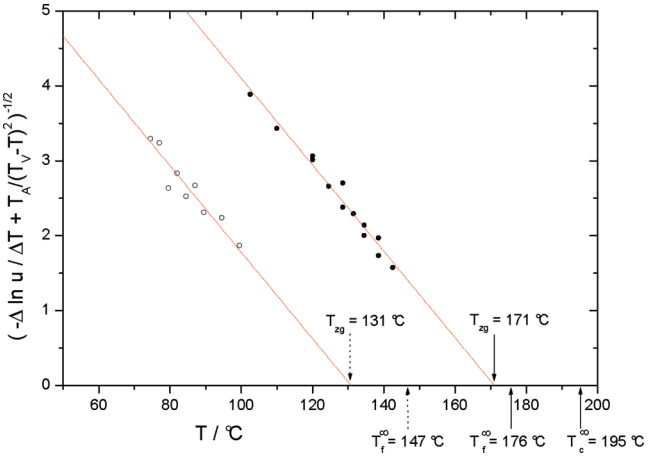


**Figure 6.** sPP and sPPcO15: determination of zero growth temperatures according to eq 14. Comparison with the respective equilibrium melting points $T_f^\infty$ and with the temperature $T_c^\infty$ which controls the crystal thickness (from Figure 1).

Figure 6 presents the result of the measurements in the form suggested by eq 14. The derivatives $\Delta \ln u/\Delta T$ obtained by the $T$-jumps experiments are referred to the mean temperature $T_c + \Delta T/2 = T_c + 2.5$ K. The parameters in the segment mobility term were chosen as $T_A = 700$ K and $T_V = 233$ K. The figure shows several clear features:

- For both samples the linear relationship predicted by eq 14 is indeed obtained.
- For both samples one finds the same slope, indicative for a common value of the parameter $T_G$

$$T_G = 300 \text{ K}$$

- Linear extrapolation yields the zero growth temperatures

$$T_{zg} = 171 \text{ °C for sPP} \quad \text{and} \quad T_{zg} = 131 \text{ °C for sPPcO15}$$

For both samples $T_{zg}$ is located below the respective equilibrium melting point $T_f^\infty$ (176 and 147 °C). The copolymer shows the larger difference between $T_{zg}$ and $T_f^\infty$.

- The figure includes also the temperature $T_c^\infty = 195$ °C, which controls the crystal thickness. It lies distinctly above all equilibrium melting points and zero growth temperatures.

Hence, we obtained a clear answer to the question treated in this work: Inclusion of counits into a polymer chain leads not only to a drop of the equilibrium melting point but also to an even larger depression of the zero growth temperature.

## 5. Data Evaluation Based on Multistage Model

We interpret the appearance of three characteristic temperatures in the laws controlling crystallization and melting of bulk polymers as indication for the inclusion of a third phase in the growth process and proposed a multistage model.[2,17] Indeed,

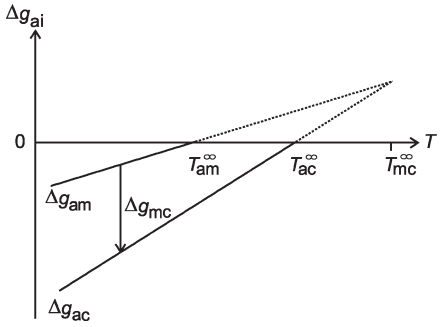


**Figure 7.** Thermodynamic conditions assumed for crystallizing polymers: temperature dependencies of the bulk chemical potentials of a mesomorphic (label m) and the crystalline phase (c). The potentials are referred to the chemical potential of the melt (a).

participation of a transient "mesophase" with a state of order intermediate between the melt and the crystal would yield a simple explanation for the existence of three controlling temperatures, as these could be identified with the transition temperatures between the three phases. The conditions under which such a mesomorphic phase can interfere are described in the scheme of Figure 7, which shows for both the crystalline phase and the mesophase the bulk chemical potential ($g_c$ and $g_m$) referred to that of the melt ($g_a$):

$$\Delta g_{ac} = g_c - g_a$$
$$\Delta g_{am} = g_m - g_a \tag{16}$$

Since the bulk chemical potential of the crystal is always below that of the mesomorphic phase, the mesophase is only metastable for macroscopic systems. However, for objects with sizes in the nanometer range stabilities can be inverted. The plot shows the three transition temperatures denoted $T_{am}^{\infty}$, $T_{ac}^{\infty}$, and $T_{mc}^{\infty}$, and they are arranged as

$$T_{am}^{\infty} < T_{ac}^{\infty} < T_{mc}^{\infty} \tag{17}$$

Thermodynamics relates $T_{am}^{\infty}$, $T_{ac}^{\infty}$, and $T_{mc}^{\infty}$ to the entropy and enthalpy increases $\Delta s_{ma}$, $\Delta s_{ca}$ and $\Delta h_{ma}$, $\Delta h_{ca}$ associated with a melting of the mesomorphic and the crystalline phase, respectively, according to the relationship

$$(T_{mc}^{\infty} - T_{ac}^{\infty})\Delta s_{ca} \approx (T_{mc}^{\infty} - T_{am}^{\infty})\Delta s_{ma} \tag{18}$$

or

$$\frac{\Delta h_{ma}}{\Delta h_{ca}} = \frac{\Delta s_{ma} T_{am}^{\infty}}{\Delta s_{ca} T_{ac}^{\infty}} \approx \frac{(T_{mc}^{\infty} - T_{ac}^{\infty}) T_{am}^{\infty}}{(T_{mc}^{\infty} - T_{am}^{\infty}) T_{ac}^{\infty}} \tag{19}$$

The equation follows from the scheme in Figure 7 using

$$\Delta s_{ca} = \frac{d\Delta g_{ac}}{dT} \quad \text{and} \quad \Delta s_{ma} = \frac{d\Delta g_{am}}{dT} \tag{20}$$

Our multistage model has been repeatedly described (see, e.g., Figure 21 in ref 3 or Figure 1 in ref 2) and is sketched here only briefly. The model assumes for the growth of polymer crystallites a specific process. The transfer of chain sequences from the melt into a growing crystallite takes place via a sequence of steps which includes passage through a mesophase. The mesophase appears in a limited zone between the lateral crystal face and the melt, stabilized by epitaxial forces. Chain sequences are first attached to the external face of the mesomorphic layer. Its thickness increases up to a critical value at which it solidifies under

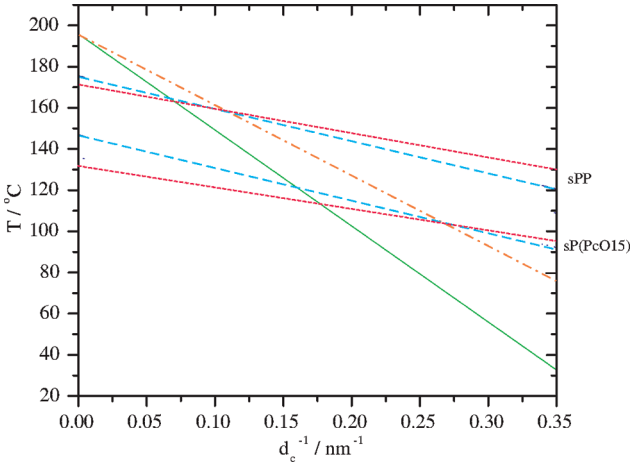


**Figure 8.** sPP and sPPcO15, $d_c^{-1}/T$ nanophase diagram with various transition lines: transition between mesophase and initial crystallites (identical with crystallization line in Figure 1, continuous), transition between mesophase and stabilized crystallites (recrystallization line taken from ref 20, dash-point), transition between stabilized crystals and melt (identical with melting lines in Figure 1, dashes), and transition between mesophase and melt (points).

formation of a crystal block. As suggested by Sirota,[18] block formation limits the surface stress arising from the mesophase to crystal densification. In a last step the block perfects in structure and increases its stability. As shown recently for poly(L-lactide), this can be achieved by an ordering of the fold surface.[19]

Application of the model in the data evaluation implies to identify the crystallization line and the melting lines in Figure 1 with transition lines in a $d_c^{-1}/T$ nanophase diagram: (i) the melting line with the thickness dependent melting point of stabilized crystallites; (ii) the crystallization line with the thickness-dependent transition between a layer with mesomorphic structure and a crystal layer in the initial, i.e., not yet stabilized, form.

The complete phase diagram includes two more thickness-dependent transition lines: (i) that between stabilized crystallites and mesomorphic layers, addressed as "recrystallization line"; (ii) the melting points of mesomorphic layers.

The first one follows from recrystallization experiments on samples crystallized at large supercooling.[20] These experience a continuous structure change up to the final melting at a characteristic fixed temperature at the crossing of the recrystallization line with the melting line. The model associates this fixed temperature with a triple point with equal values of the chemical potentials of the melt, the mesomorphic layer, and stabilized crystallites. The melting line of the mesomorphic layers can also be plotted since two points are known: (i) $T_{zg}$ is identical with the equilibrium melting point of the mesophase, i.e., the melting point in the macroscopic limit $d_c^{-1} \to 0$. (ii) The transition line passes through the just mentioned triple point.

Figure 8 depicts the thus-completed nanophase diagram showing the transition lines for both the homopolymer and the chosen copolymer. As we see, the lines referring to the transition between mesomorphic layers and the melt for the two materials have practically the same slope. The slope is again given by the Gibbs−Thomson eq 3 and, hence, by the ratio $2\sigma_{am}T_{zg}/\Delta h_{am}$. Here $\Delta h_{am}$ denotes the macroscopic heat of melting of the mesophase, and $\sigma_{am}$ describes the surface free energy of mesomorphic layers. $\Delta h_{am}$ can be determined by applying eq 19. For sPP we obtain $\Delta h_{am}/\Delta h_{ac} = 0.79$, and for sPPcO15 the result is $\Delta h_{am}/\Delta h_{ac} = 0.75$. Both results are virtually identical. The deviations from the average value

$$\Delta h_{am}/\Delta h_{ac} = 0.77$$

lie within the error limits of the experiment. Choosing for the heat of fusion of sPP the literature value $\Delta h_{ac} = 7.7$ kJ/mol $C_3H_6$, we obtain for the mesophase a heat of fusion $\Delta h_{am} = 5.9$ kJ/mol $C_3H_6$ and a surface free energy $\sigma_{am} = 3.7$ kJ/mol. In fact, all these result confirm values obtained already a couple of years ago based on other observations and arguments (see Table 2 in ref 21).

The observation of a larger effect of the counits on the melting point of the mesophase than for the crystals—40 K compared to 30 K—comes as expected, considering Raoult's law. Under ideal conditions the melting point depression is inversely proportional to the heat of fusion. Exactly this is found here, even in the right proportion

$$30\ \mathrm{K}/40\ \mathrm{K} = 0.75 \approx \Delta h_{am}/\Delta h_{ac}$$

Considering the exponential temperature dependence of the crystal growth rate, eq 2, the process must include some activation step. In the framework of the multistage model we proposed the following:[2] Before a sequence, which lies coiled in the melt, is incorporated into the growing mesomorphic layer, it has to be activated by a transfer into the overall straightened form required for an attachment. This straightening has to reach at least the length set by the initial thickness of the mesomorphic layer. The associated increase in the conformational free energy, $\Delta F^{con}$, is proportional to the number $n$ of monomers in the sequence, and we write

$$\Delta F^{con} = n\Delta f^{con}$$

Theory yields the following expression for the activation energy per monomer $\Delta f^{con}$ (eqs 32 and 35 in ref 2):

$$\Delta f^{con} = \frac{R\Delta h_{am} T_G}{2\sigma_{am}} \tag{21}$$

Since $T_G$ has been measured (573 K), we can determine the activation energy per monomer. It amounts to

$$\Delta f^{con} = 3.8\ \frac{\mathrm{kJ}}{\mathrm{mol}\ C_3H_6}$$

**Acknowledgment.** Support of this work by the Deutsche Forschungsgemeinschaft is gratefully acknowledged. Thanks are also due to the "Fonds der Chemischen Industrie" for the generous help provided over many years.

## References and Notes

(1) Hoffman, J.; Davis, G.; Lauritzen, J. In *Treatise on Solid State Chemistry*; Hannay, N. B., Ed.; Plenum: New York, 1976; Vol. *3*.
(2) Strobl, G.; Cho, T. *Eur. Phys. J. E* **2007**, *23*, 55.
(3) Strobl, G. *Rev. Mod. Phys.* **2009**, *81*, 1287.
(4) Hauser, G.; Schmidtke, J.; Strobl, G. *Macromolecules* **1998**, *31*, 6250.
(5) Cho, T.; Heck, B.; Strobl, G. *Colloid Polym. Sci.* **2004**, *282*, 825.
(6) Cho, T.; Stille, W.; Strobl, G. *Colloid Polym. Sci.* **2007**, *285*, 931.
(7) Cho, T.; Stille, W.; Strobl, G. *Macromolecules* **2007**, *40*, 2590.
(8) Thomann, R.; Wang, C.; Kressler, J.; Juengling, S.; Muelhaupt, R. *Polymer* **1995**, *36*, 3795.
(9) Fritsch, J.; Stille, W.; Strobl, G. *Colloid Polym. Sci.* **2006**, *284*, 620.
(10) Hawkins, S.; Richards, R. *J. Polym. Sci.* **1949**, *4*, 515.
(11) Keane, J.; Stein, R. *J. Polym. Sci.* **1956**, *20*, 327.
(12) Levy, B. *J. Appl. Polym. Sci.* **1961**, *5*, 408.
(13) Mahen, K.; James, W.; Bosch, W. *J. Appl. Polym. Sci.* **1965**, *9*, 3605.
(14) Kerker, M. *The Scattering of Light*; Academic Press: New York, 1969; p 418.
(15) Heck, B.; Kawai, T.; Strobl, G. *Polymer* **2006**, *47*, 5538.
(16) Fritsch, J. Diplomarbeit, Physikalisches Institut, Universitaet Freiburg, 2005.
(17) Strobl, G. *Eur. Phys. J. E* **2000**, *3*, 165.
(18) Sirota, E. *Macromolecules* **2007**, *40*, 1043.
(19) Cho, T.; Heck, B.; Strobl, G. *Chin. J. Polym. Sci.* **2007**, *25*, 83.
(20) Heck, B.; Siegenfuehr, S.; Strobl, G.; Thomann, R. *Polymer* **2007**, *48*, 1352.
(21) Strobl, G. *Eur. Phys. J. E* **2005**, *18*, 295.